Hybrid neural network bushing model for vehicle dynamics simulation [†]

Jeong-Hyun Sohn[1], Seung-Kyu Lee[2] and Wan-Suk Yoo[3,*]

[1]*School of Mechanical Engineering, Pukyong National University, San 100, Yongdang-dong, Nam-gu, Busan, 608-739, Korea*
[2]*Power & Industrial System R&D Center, Hyosung Corporation*
454-2, Nae-Dong, Changwon, Gyeongsangnam-Do, 641-712, Korea
[3]*School of Mechanical Engineering, Pusan National University, San 30, Jangjeon-dong, Geumjung-gu, Busan, 609-735, Korea*

───

Abstract

Although the linear model was widely used for the bushing model in vehicle suspension systems, it could not express the nonlinear characteristics of bushing in terms of the amplitude and the frequency. An artificial neural network model was suggested to consider the hysteretic responses of bushings. This model, however, often diverges due to the uncertainties of the neural network under the unexpected excitation inputs. In this paper, a hybrid neural network bushing model combining linear and neural network is suggested. A linear model was employed to represent linear stiffness and damping effects, and the artificial neural network algorithm was adopted to take into account the hysteretic responses. A rubber test was performed to capture bushing characteristics, where sine excitation with different frequencies and amplitudes is applied. Random test results were used to update the weighting factors of the neural network model. It is proven that the proposed model has more robust characteristics than a simple neural network model under step excitation input. A full car simulation was carried out to verify the proposed bushing models. It was shown that the hybrid model results are almost identical to the linear model under several maneuvers.

Keywords: Bushing; linear model; Neural network; Vehicle dynamics simulation; Hysteresis

───

1. Introduction

The bushing element is a hollow cylinder connecting the outer steel cylindrical sleeve and the inner steel cylindrical rod. The inner rod is connected to the chassis frame and used to transfer forces from the wheel to the chassis frame. Due to the rubber materials in the bushing, it has nonlinear characteristics in terms of load amplitudes and frequencies, and hysteresis. Since the characteristics of the rubber bushing significantly affect the accuracy of the vehicle dynamic simulation, it should be accurately modeled.

The bushing forces depend not only on the instantaneous deformation but also on the past history of deformation. As a result, the hysteretic restoring force cannot be expressed by instantaneous displacement and velocity. This history-dependent characteristic of bushing makes it more difficult to model and analyze hysteretic systems.

In commercial multi-body simulation programs, the linear model was widely used for the bushing element. This model treats the bushing element as a linear combination of three translational spring-dampers and three rotational spring-dampers. However, this type of bushing model cannot properly generate the hysteretic behavior of the bushing element.

To get an accurate bushing model, a black-box approach was used. The technique of empirical modeling based on the neural network approach is able to describe both the amplitude-dependent and frequency-dependent nonlinearities. The modeling is not based on any physical law but uses powerful mathe-

matical tools to describe the behavior of complex systems. In principle, neural networks are simple algebraic functions containing many parameters. By applying gradient-based optimization algorithms, the neural network parameters can be adjusted to simulate the behavior of the system. As no differential equation is involved in the system, the neural network model is numerically efficient; however, it has some drawbacks in that it is difficult to interpret the physical meaning of the results.

The bushing modeling using neural networks has been used by some researchers. Barber [1] studied the possibility of the artificial neural network for modeling the bushing. Sohn et al. [2] did vehicle dynamic simulations using the neural network-based bushing model. The main issue is how to achieve accurate data approximation over a wide range of frequencies and amplitudes achieved at the same time.

The main purpose of this paper is to develop a neural network-based hybrid bushing model for overcoming the instability of neural network model and accurately carrying out the full car simulation.

2. Neural network models

2.1 linear model

The linear model can be represented by a viscous damper and elastic spring connected in parallel as shown in Fig. 1. The output force can be calculated as follows:

$$F = k_o x + c_o \dot{x} \qquad (1)$$

where k_0 and c_0 indicate the spring stiffness and damping coefficient, respectively. The parameter x is the spring deformation and $\dot{x}$ is the time derivative of deformation.
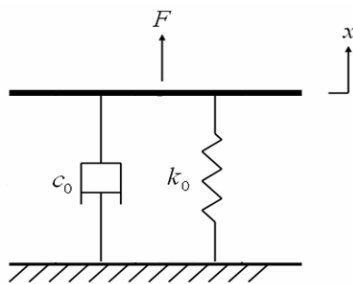
ADAMS and RecurDyn adopt the linear model for the bushing element. This model represents the bushing element as the linear combination of three translational spring-dampers and three rotational spring-dampers. Bushing forces in the linear model can be calculated as follows:

$$F_q = K_q q + c_q \dot{q} \qquad q = x, y, z \qquad (2)$$

$$T_q = K_{\theta q}\theta_q + c_{\theta q}\dot{\theta}_q \qquad q = x, y, z , \quad \theta_q = \theta_x, \theta_y, \theta_z \qquad (3)$$

where F_q denotes the translational forces and T_q means the rotational moments. K_q, c_q indicate translational spring stiffness and damping coefficient along the x, y, and z axis, and $K_{\theta_q}, c_{\theta_q}$ are rotational spring stiffness and damping coefficient about the x, y, and z axis.

2.2 Neural network model

The neural network structure with multiple inputs is shown in Fig. 2. The neuron collects the signals from all the inputs and multiplies them by weight factors. Then, an internal signal is built as the sum of the weighted inputs and a bias value is written by the Eq. (4).

$$\sum n_{i1} = w_{i1}x_1 + w_{i2}x_1 + \cdots + w_{ip}x_1 + b_i = \sum_{j=1}^{p} w_{ij}x_j + b_i$$

$$= \mathbf{W}_i \mathbf{x} + b_i \qquad (4)$$

where the index i denotes the numbering of the neuron. The output of a neuron of hidden layer is written as:

$$a_i^1 = f_i(n_{i1}) \qquad (5)$$

Fig. 1. linear model.
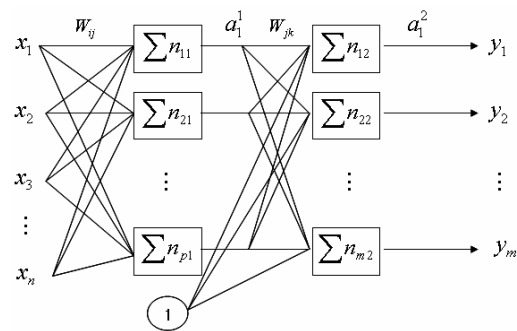
Fig. 2. Neural network structure.

The activation function f_i defines the sensitivity of the neuron according to the external stimulation. As the activation functions, a sigmoid function, a hyperbolic tangent sigmoid function, and a linear function are commonly used.

The layer directly connected to the output is called the output layer and the remaining ones are called hidden layers. The outputs of the network are described as a composite function of the individual layers. The network function is determined by both the weighting factors and the bias values. The network parameters contain information about the system behavior and have to be set or identified correctly if the network has to solve a given problem with sufficient accuracy.

The weight factors are updated on the basis of a comparison between the actual calculated output and its associated or given target. This algorithm is executed in the loop until the network output matches the target exactly or with sufficient approximation. The accuracy of approximation is given by the squared error performance function E as:

$$E = \sum_{k=1}^{N} |\mathbf{e}(k)|^2 = \sum_{k=1}^{N} |\mathbf{t}(k) - \mathbf{a}(k)|^2 \qquad (6)$$

where a(k) is the actual output, t(k) the corresponding calculated output and N the number of used input-target pairs. The back propagation algorithm refers to the method of computing the gradient of the squared error function with respect to all the weights and biases by the application of the chain rule [3].

3. Hybrid bushing model

In a neural network model, the information about the system behavior is stored in both the weighting factors and the biases, which have no physical meanings. In this study, the total bushing forces are composed of two components, F_{lin} and F_{nn}. The first component F_{lin} is the force from the linear model and describes the linear part of the bushing characteristics, which is called 'backbone' in this paper. The second one, F_{nn}, represents the force from the neural network wrapped around the linear model backbone, representing all the remaining effects occurring in the system, mainly the frequency-dependent hysteresis. Fig. 3 represents the structure of the hybrid bushing model.

The neural network bushing model is proposed to take into consideration both the hysteresis and the nonlinearities of frequency and displacement of rubber based on the dynamic test results of the rubber bushing elements. Since the rubber bush has hysteretic characteristics, the inputs and outputs of the previous steps affect the current outputs. Therefore, inputs and outputs of the past are used as the input data of the current step. The input components of the neural network are selected from the current displacement, the past displacement and the past outputs. The value of the output layer is the rubber bush force. The structure of the model and the number of neurons of hidden layers were set as shown in Fig. 3. In this study, only one hidden layer with a hyperbolic tangent sigmoid function is used. For the output layer, a linear function is applied to enable the network output to take any real positive or negative value.

Fig. 4 represents the deformations of the bushing element between two bodies. The deformation of the rubber bushing can be represented as the following equation:
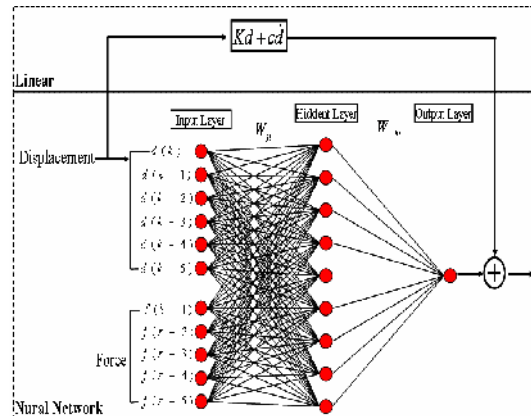
Fig. 3. Structure of the combined model used in this study.
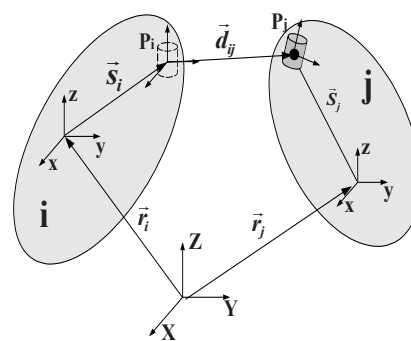
Fig. 4. Deformation between bushing points P_i and P_j.
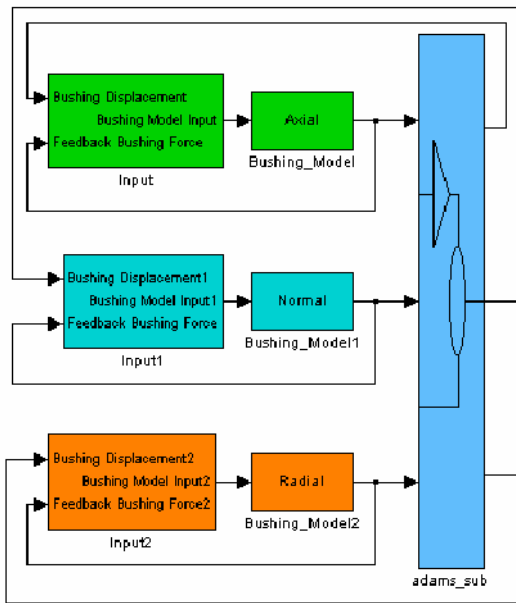
Fig. 5. Structure of interface between ADAMS and MATLAB.

$$\mathbf{d}_{ij} = \mathbf{r}_j + \mathbf{s}_j - \mathbf{r}_i - \mathbf{s}_i \qquad (7)$$

where $\mathbf{r}_i$, $\mathbf{r}_j$ are position vectors from the inertial reference frame to the body coordinate system of body i and body j, respectively. The vectors $\mathbf{s}_i$, $\mathbf{s}_j$ are the position vectors of the bushing points P_i and P_j in the body coordinate system, respectively.

To calculate the bushing forces in the ADAMS program under the SIMULINK environment, bushing deformation data are transferred to MATLAB. Then, MATLAB calculates bushing forces and these data are used for the next time step in the ADAMS program. To consider the displacement history-dependent bushing, a special routine is required for data storage and linear interpolation of the past integration steps. Therefore, a code which is written in MATLAB has been developed, which supplies the hybrid model with the correct input data and calculates the current bushing forces. To use the hybrid bushing model in the ADAMS program, an interface module is developed in this study. Fig. 5 shows the structure of the interface between ADAMS and MATLAB under Simulink environment. The procedure for calculating bushing forces is shown in Fig. 6. At the first step, the bushing deformations and velocities are calculated in ADAMS. They are transferred to MATLAB through the input block of SIMULINK. In
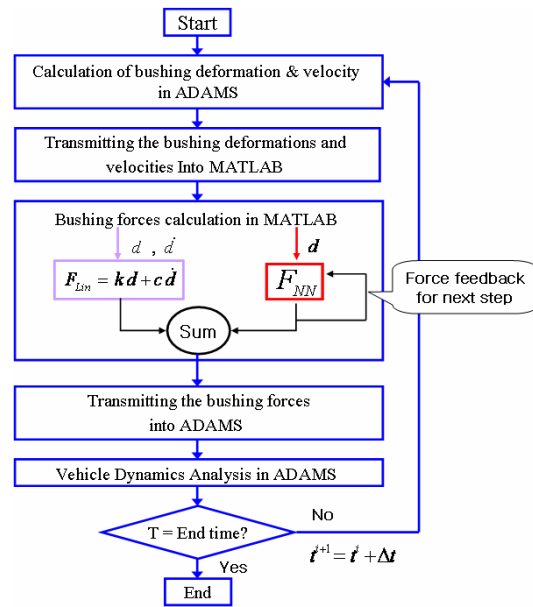
Fig. 6. Flow chart for the bushing force calculation.

MATLAB, F_{lin} are calculated by using the current deformation and velocity. From the current information and past information, F_{NN} can be calculated. The resultant forces are transmitted to ADAMS. The SFORCE element of ADAMS is used for the bushing forces. The dynamic equations are solved in ADAMS and then the next bushing deformation and velocity are calculated for the next step. Until the time meets "end" this process is repeated.

4. Identification of the hybrid model

4.1 Identification of the linear model characteristics

Fig. 7 shows the bushing coordinate system. Random excitation tests using MTS 3-axes rubber testing machine as shown in Fig. 8 are carried out to obtain the bushing characteristics [4]. The machine can excite 3-directional (axial, normal, and radial) motion at the same time. Figs. 9 and 10 represent the radial and axial bushing forces under the random excitation inputs, respectively.

The random excitation input data were generated by using RPCⅢ software supported by MTS, Inc. The RPCⅢ system has the following sampling rates: 51.2, 64, 102.4, 204.8, 256, 409.6, 512, 1024, 2048 Hz. Since a sampling rate of 204.8 Hz was chosen with a frame size of 1024 points per frame, the time interval was calculated as 0.0049.

The bushing stiffness and damping coefficient
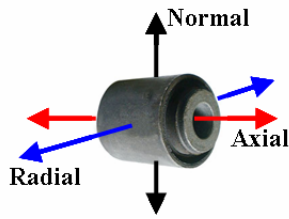
Fig. 7. Bushing coordinate system.

Fig. 8. Bushing test using MTS 3-axes tester.
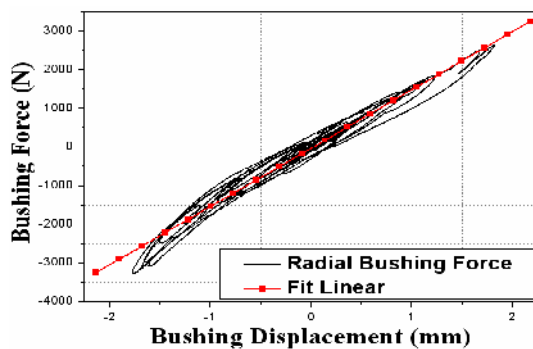
Fig. 9. Radial bushing force under random input.
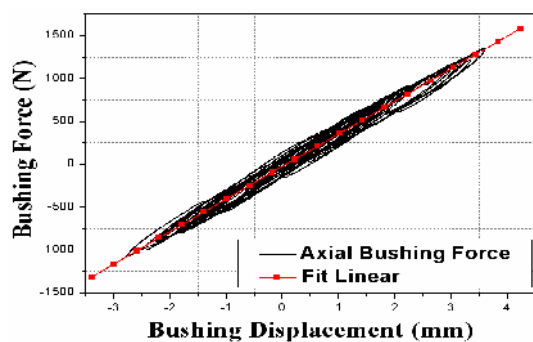
Fig. 10. Axial bushing force under random input.

Table 1. Bushing stiffness and damping coefficients.

Direction	Stiffness [N/mm]	Damping [Ns/mm]
Radial	1518.73	15
Axial	379.68	4.4

changes as the amplitude and frequency change. In this study, the bushing stiffness is calculated through the linear fit as shown in Fig. 9 and Fig. 10. To obtain damping coefficients, harmonic tests with an amplitude of 2 mm, frequency of 10 Hz for radial damping coefficient and test with amplitude of 3 mm, frequency of 10 Hz for axial damping coefficient are performed.

The radial and axial stiffness and damping coefficients are represented in Table 1.

4.2 Identification of the neural network parameters

Random test data are split into training and prediction data sets. The prediction set should remain unseen by the network to enable verification. Only the training set is presented to the network within the training phase. The experimental data are scaled before training into the range between -1 and +1. This improves the convergence behavior of the training algorithm. The general procedure is to train the network by using a training data set and to see how well the generalization is on a prediction set. It is an iterative process.

Since the bushing has hysteretic characteristics, the inputs and outputs of the previous steps affect the current outputs. Therefore, inputs and outputs of the past are used as the input data of the current step. The input components of the neural network are selected from the current displacement, past displacements, and past bushing forces. The value of the output layer is the bushing force. Through a trial-and-error process, the past five displacements and past five forces and one hidden layer with nine neurons are used as shown in Fig. 4.

The simulation results using unseen data sets are compared to the experimental results. Table 2 represents the prediction errors. In the table2, Linear is the linear model, NN means the pure neural network model, and Hybrid indicates the hybrid model, respectively. The RMS and MAX in the table 2 represent the root mean square errors and maximum errors, respectively.

As shown in table 2, the linear model has more

Table 2. Comparison of prediction error (%).

	Axial			Radial		
	Linear	NN	Hybrid	Linear	NN	Hybrid
RMS	9.8	5.1	4.8	11.9	4.3	4.6
MAX	13.7	7.7	7.5	20.1	8.8	9.1

errors than the others, and the NN model shows similar results with the hybrid results. It is shown that the errors of the hybrid model are less than 10% compared to the experimental results under random excitation. Therefore, the hybrid model can be acceptable as the accurate bushing model with stability for vehicle dynamics simulation.

5. Numerical examples

5.1 3-axes bushing test

Fig. 11 shows the ADAMS model for 3-axes bushing test. The random excitation inputs of the axial, radial, and normal direction are imposed on the bushing simultaneously. Fig. 12 and Fig. 13 represent the axial and radial bushing forces, respectively. We compared the simulation results with the experimental results. Table 3 shows the comparison of errors. In Table 3, the RMS ratio as written by the Eq. (8) is the ratio between the RMS (root mean square) of the experiment result and the RMS of the simulation error. ESR as shown in Eq. (9) is the error-to-signal-ratio of the estimated model. As a matter of fact, it is the ratio between the variance of the estimation error and the variance of the output. ESR lies in the range from 0 to 1; ESR=1 means that the model only predicts the average value of the output. ESR=0 means that the model exactly predicts the output of the system.

$$\text{RMS ratio} = \frac{\sqrt{\frac{1}{T}\sum_{t=1}^{T}(F_{\exp}(t)-F_{pre}(t))^2}}{\sqrt{\frac{1}{T}\sum_{t=1}^{T}(F_{\exp}(t))^2}} \tag{8}$$

$$\text{ESR} = \frac{\frac{1}{T}\sum_{t=1}^{T}(F_{\exp}(t)-F_{pre}(t))^2}{\frac{1}{T}\sum_{t=1}^{T}(F_{\exp}(t)-(\frac{1}{T}\sum_{i=1}^{T}F_{\exp}(i)))^2} \tag{9}$$

As shown in Table 3, the RMS ratio of the linear model is about two times compared to the hybrid model and the maximum error is more than two times. The NN model shows similar results to the hybrid

Table 3. Comparisons of errors (%).

	Axial			Radial		
	linear	NN	Hybrid	linear	NN	Hybrid
RMS ratio	10.9	5.2	5.1	5.1	3.0	3.0
ESR	0.5	0.2	0.2	0.4	0.2	0.2
MAX	24.9	9.3	8.4	20.7	8.3	7.8
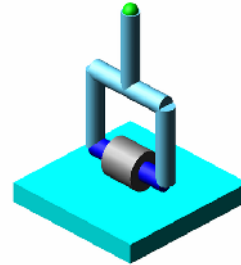
Fig. 11. ADAMS model for a 3-axes bushing test.
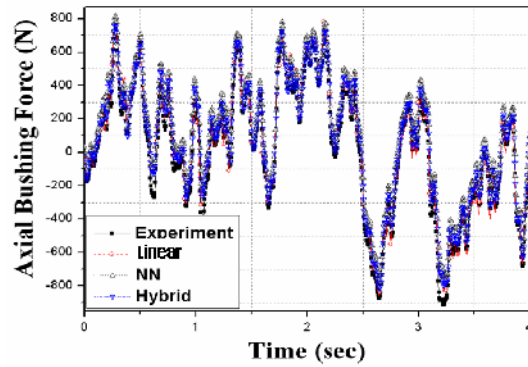
Fig. 12. Axial bushing forces.
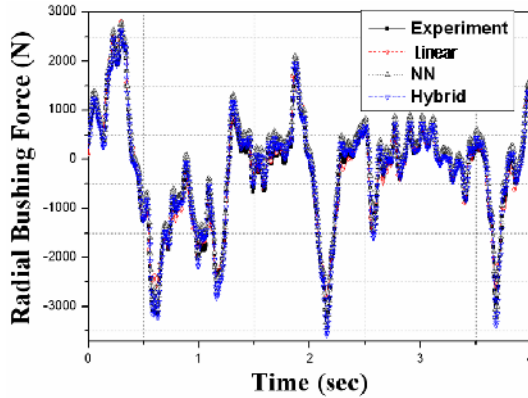
Fig. 13. Radial bushing forces.

model. The errors of the hybrid model are within 10% compared to the experimental results.
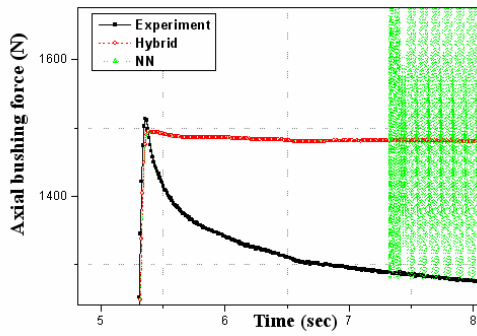
Fig. 14. Axial bushing forces.

5.2 Step input test and simulation

To investigate the difference between the neural network model and the hybrid model, a 4 mm step input excitation simulation is performed. Fig. 14 shows the axial bushing forces. Experimental results show well the relaxation phenomenon according to time; however, simulation results do not represent it correctly. In particular, the neural network model (NN) diverges after 7.3 sec. This shows the instability of the neural network model under an unexpected excitation input. In this paper, a hybrid model is suggested to overcome this phenomenon and obtain stable responses.

5.3 Full car simulation

To demonstrate the validity of the proposed bushing model, a full-car simulation is performed as shown in Fig. 15. The ADAMS program is employed to model the full car. The full car model consists of a front and a rear suspension, a front and a rear stabilizer bar, a steering system, a differential gear, and a frame. The front suspension is double-wishbone type suspension and a rear suspension is 5-link type suspension. The total degrees of freedom are 78. The UA tire model in the ADAMS program is used and the suspension spring is modeled as a linear spring element, and damping characteristics of the suspension are approximated into the spline function. The bushing connecting the upper control arm and the frame is taken in hybrid model into account as shown in the left upper corner of Fig. 15. The direction of the axial bushing force is the longitudinal of the vehicle, the radial direction is the lateral, and the normal direction is the vertical. A pulse steer simulation and pot hole running simulation are carried out for the validation of the proposed model.
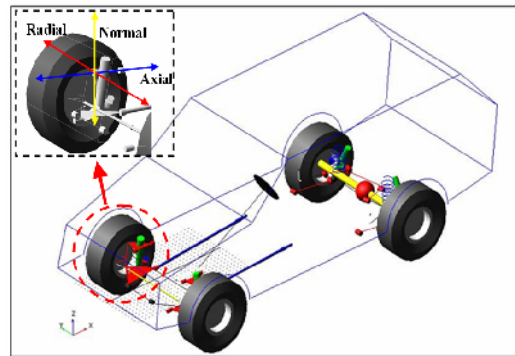
Fig. 15. Full car model.
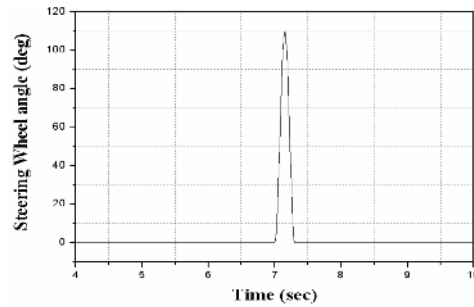
Fig. 16. Steering wheel angle for pulse steer simulation.

5.3.1 Pulse steer simulation

Fig. 16 shows the steering wheel angle for pulse input maneuver. The initial velocity is 30 km/h. The front upper control arm bushing forces are compared in Figs. 17-19. As shown in the figures, the linear model shows good agreement with the hybrid model. This is because the maximum bushing force is within the linear region. As shown in Fig. 17, a peak difference between the hybrid and linear model at 7.15 sec is about 6.5 N (16.9%). In Fig. 18 and Fig. 19, peak differences are about 15 N (2.1%) and 4 N (3.6%), respectively.

5.3.2 Pothole running simulation

Fig. 20 shows the pothole shape. The initial velocity of the vehicle is 30 km/h. Bushing forces at the front upper control arm under the pothole simulation are compared in Figs. 21-23. As shown in the figures, the linear model shows good agreement with the hybrid model. However, in the case of the normal direction, a peak difference between the linear model and the hybrid model is about 215 N. This is because the maximum bushing force is over the linear region (about 2000 N).
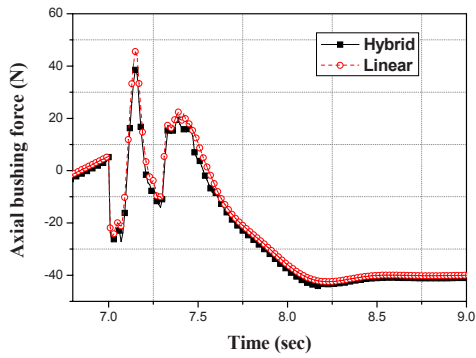
Fig. 17. Axial bushing force for pulse input simulation.
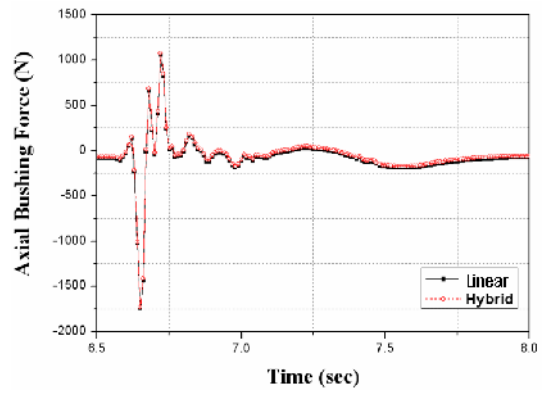
Fig. 21. Axial bushing force for pothole simulation.
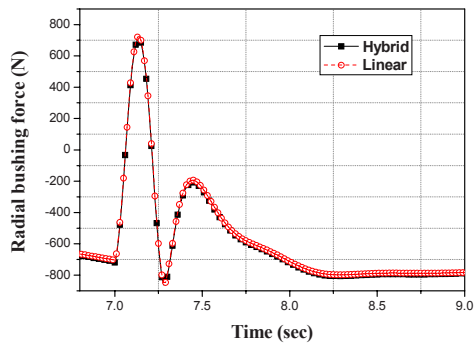
Fig. 18. Radial bushing force for pulse input simulation.
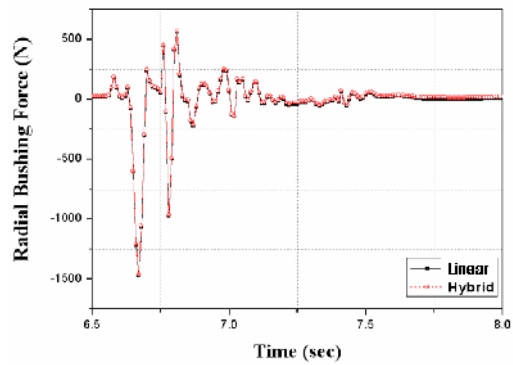
Fig. 22. Radial bushing force for pothole simulation.
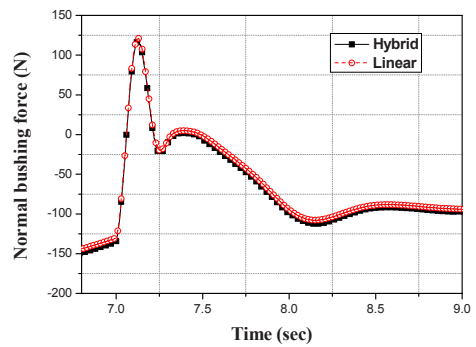
Fig. 19. Normal bushing force for pulse input simulation.
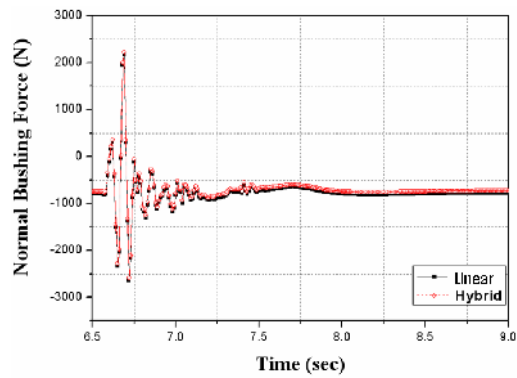
Fig. 23. Normal bushing force for pothole simulation.
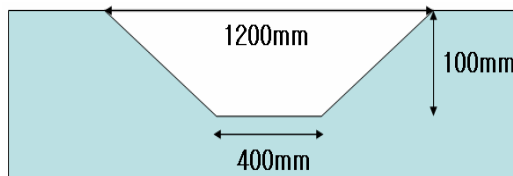
Fig. 20. Pothole shape.

5.3.3 Fishhook simulation

Fig. 24 shows the steer input angle, and Fig. 25 represents the configuration of the chassis frame under fishhook maneuver. Bushing forces at the front upper control arm of the fishhook simulation are
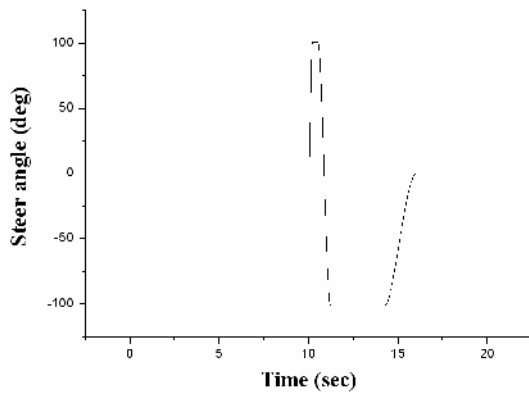
Fig. 24. Steer angle.
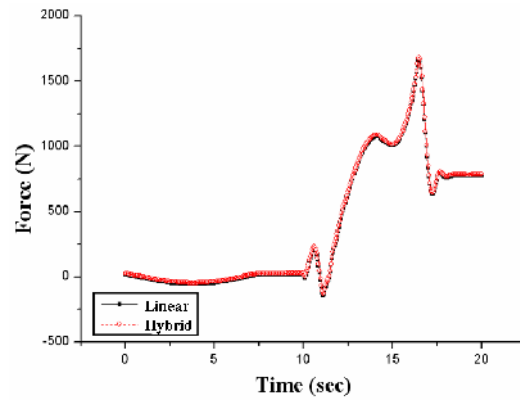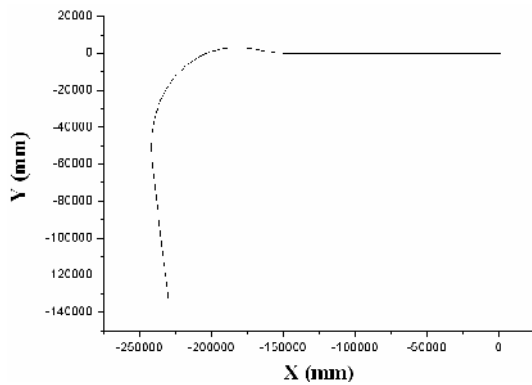
Fig. 25. Configuration of chassis frame for fishhook simulation.
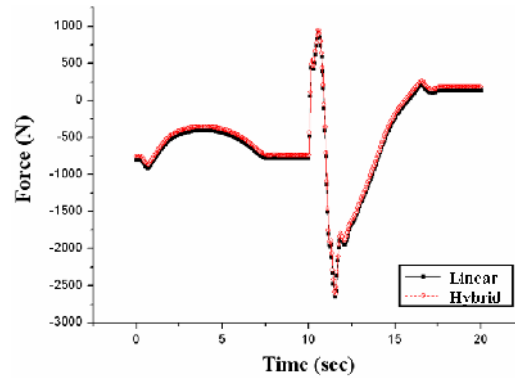
Fig. 26. Axial bushing force for fishhook simulation.

compared in Figs. 26-28. As shown in the figures, the hybrid model does not diverge and shows similar results to the linear model.

Fig. 27. Radial bushing force for fishhook simulation.

Fig. 28. Normal bushing force for fishhook simulation.

6. Conclusions

In this paper, a hybrid neural network bushing model is suggested that was developed on the basis of two different modeling techniques and can be used in ADAMS. The linear model is used to create the backbone of the bushing model, and the neural network model is used to describe the nonlinear hysteretic characteristics. Combining the advantages of both the linear model and the neural network approach, the hybrid bushing model is able to represent the complex behavior of experimental force-displacement data, including history-dependent hysteresis phenomena.

The proposed hybrid modeling technique was validated by dynamic analyses of a 3-axes bushing model and a full car simulation. The numerical results were compared with the conventional linear model, the pure neural network model, and experimental results. As a result, a pure neural network model shows good results compared to the experimental results. How-

ever, it shows undesirable responses under unexpected step excitation input. The hybrid bushing model has more stable responses than a neural network model because of the linear model's so-called backbone model. Therefore, this model is available to carry out vehicle dynamics simulation under versatile maneuvering with stability. It will need to be compared with the full car test results in the future.

References

[1] A. J. barber, Accurate Models for Complex Vehicle Components using Empirical Methods, *SAE paper* No. 2000-01-1625, 2000.

[2] J. H. Sohn, S. K. Lee, J. K. Ok and W. S. Yoo, Comparison of semi-physical and black-box bushing model for vehicle dynamics simulation, *Journal of Mechanical Science and Technology*, 21, No. 2, 264-271, 2007.

[3] K. S. Narendra and K Parthasarathy, Identification and Control of Dynamic System Using Neural Networks, *IEEE Transactions on Neural Networks*, 1(1), 4-27, 1990.

[4] E. Y. Kuo, Testing and Characterization of Elastomeric Bushing for Large Deflection Behavior, *SAE Technical report*, No. 970099, 1997.

Dr. Wan-Suk Yoo was born in 1954, and received B.S. degree from Seoul National University (1976), and got M.S. degree from KAIST (1978) and Ph.D. from the University of Iowa (1985). He is currently a full professor at the Pusan National University in Korea, where he joined since 1978. His major area is vehicle dynamics and flexible multibody dynamics. He became an ASME Fellow (2004), and currently serving as an associate editor for the ASME, J. of computational and nonlinear dynamics. He is also serving a contributing editor for the multibody system dynamics journal. He is serving as ISC chair for the ACMD2008, and a member at IFToMM TC for multibody dynamics. He is currently a vice-president of the KSME (Korean Society of Mechanical Engineers).